JOC The Journal of Organic Chemistry

Featured Article

pubs.acs.org/joc

Structural, Optical, and Electrochemical Properties of Three-Dimensional Push−Pull Corannulenes

Yi-Lin Wu,[†] Mihaiela C. Stuparu,[‡] Corinne Boudon,[§] Jean-Paul Gisselbrecht,[§] W. Bernd Schweizer,[†] Kim K. Baldridge,*[,‡] Jay S. Siegel,*[,‡] and François Diederich*[,†]

[†]Laboratorium für Organische Chemie, ETH Zürich, Hönggerberg, HCI, 8093 Zürich, Switzerland

[‡]Institute of Organic Chemistry, University of Zürich, Winterthurerstrasse 190, 8057 Zürich, Switzerland

[§]Laboratoire d'Electrochimie et de Chimie Physique du Corps Solide, UMR 7177 CNRS, Université de Strasbourg, 4 rue Blaise Pascal, 67081 Strasbourg Cedex, France

Supporting Information

ABSTRACT: Electrochemically active corannulene derivatives with various numbers of electron-donating 4-(*N*,*N*-dimethylamino)phenylethynyl (**1**−**4**) or electron-withdrawing cyanobutadienyl peripheral substitutents (**5**−**8**) were prepared. The latter derivatives resulted from formal [2 + 2] cycloaddition of cyanoolefins to **1**−**4** followed by retro-electrocyclization. Conformational properties were examined by variable-temperature NMR and X-ray diffraction and opto-electronic properties by electronic absorption/emission spectra and electrochemical measurements; these analyses were corroborated by dispersion-corrected density functional calculations at the level of B97-D/def2-TZVPP. In CH_2Cl_2, **1**−**4** exhibit intramolecular charge-transfer (ICT) absorptions at 350−550 nm and green ($\lambda_{em} \sim 540$ nm) or orange (600 nm) fluorescence with high quantum yields (56−98%) and are more readily reduced than corannulene by up to 490 mV. The variation of optical gap and redox potentials of **1**−**4** does not correlate with the number of substituents. Cyanobutadienyl corannulenes **5**−**8** show red-shifted ICT absorptions with end-absorptions approaching 800 nm. Intersubstituent interactions lead to distortions of the corannulene core and lower the molecular symmetry. NMR, X-ray, and computational studies on **5** and **8** with one cyanobutadienyl substituent suggested the formation of intermolecular corannulene dimers. Bowl-inversion barriers around $\Delta G^{\ddagger}$ = 10−11 kcal/mol were determined for these two molecules.

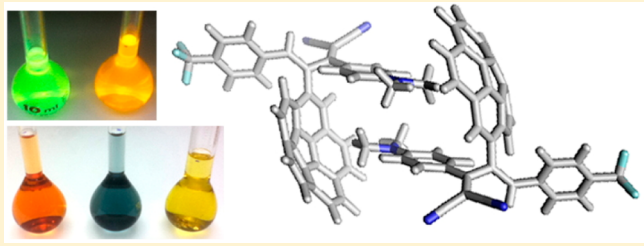

INTRODUCTION

Polycyclic aromatic organic molecules have been important components in the search for highly efficient organic (opto-)electronic devices.[1] Their large π-surfaces enable regular solid-state packing and electron transduction; the extended π-conjugation is responsible for molecular electrical and/or opto-electronic properties, which are translated into the characteristics of the bulk materials and are easily tailored by alteration of the substituents on the periphery of the π-frameworks.

Corannulene is composed of five benzene rings fused to a central five-membered cycle and has a bowl-shaped π-conjugated system, adding one more dimension to the chemistry of usually planar polycyclic aromatics.[2] In addition to the interest in the dynamic stereochemistry[3] and organometallic coordination[3d,4] associated with this curved structure, there has been growing attention to the materials applications of corannulene. For instance, lithium can be stored/intercalated between corannulenes, yielding a promising anode material for batteries.[5] A dramatic increase in fluorescence quantum yields from 0.03 to 0.8−0.9 was effected by arylethynylation of corannulene,[6] and wavelength-tunable electrochemiluminescence was achieved by forming exciplexes with coreactants during electrochemical processes.[7]

Modification of the peripheral substituents provided the electrochemically active corannulenes **1**−**8** in this work. The 4-(*N*,*N*-dimethylamino)phenylethynyl derivatives **1**−**4** constitute a new class of electron-rich and highly fluorescent corannulenes in which the anilinoethynyl substituents extend radially in a starburst fashion with limited degrees of conformational freedom. Reaction of **1**−**4** with tetracyanoethene (TCNE) or 2-[4-(trifluoromethyl)benzylidene]malononitrile proceeds by formal [2 + 2] cycloaddition (CA) between the electron-deficient alkenes and the donor-activated acetylenes, followed by retro-electrocyclization (RE), to yield a contrasting family of electron-poor corannulenes (**5**−**8**) with multiple cyanobuta-1,3-dienyl arms (Chart 1).[8]

The additional *s-cis*/*s-trans* conformational variability of the cyanobutadienyl arms in **5**−**8** further modifies the three-dimensional geometry of corannulene and allows for core-convergent as well as core-divergent geometries. A recent conformational study on nascent 2,3-diphenylbuta-1,3-diene by single-crystal X-ray analysis and MP2/6-311++G** calculations[9] revealed the preference to the synclinal conformer (torsion angle 55.6° by X-ray).[10] The corresponding anticlinal conformer

Received: October 9, 2012
Published: November 21, 2012

dx.doi.org/10.1021/jo302217n | *J. Org. Chem.* 2012, 77, 11014−11026

Chart 1. Corannulene Derivatives 1−8 with Electrochemically Active Peripheral Substituents

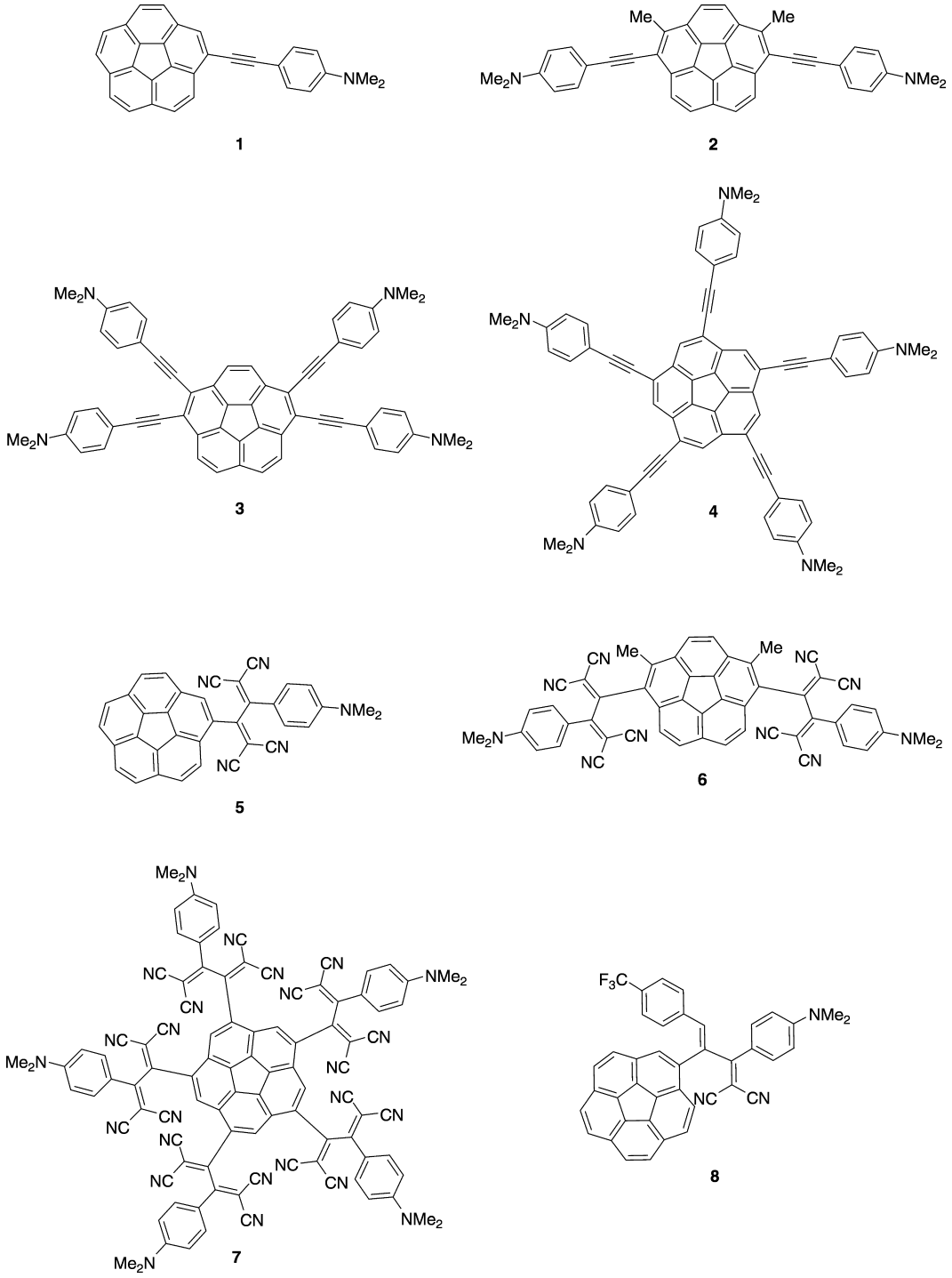

(a local minimum, torsion angle 155°) is higher in energy by 1.70 kcal/mol, and the barrier for converting the low energy conformer into the high energy one is 5.33 kcal/mol. Installation of the cyanobutadiene motifs on the periphery of corannulenes **5**−**8** is expected to introduce intersubstituent and/or substituent−corannulene interactions that influence the materials properties displayed by this family of chromophores.

RESULTS AND DISCUSSION

Synthesis. Previously reported bromo-,[6b,11] 1,6-dibromo-,[6c] 1,2,5,6-tetrabromo-,[12] and 1,3,5,7,9-pentachlorocorannulenes[11,13] allowed access to the peripherally functionalized, electrochemically active corannulenes. Mono- and bis[4-(dimethylamino)phenylethynyl]corannulenes **1** and **2** were prepared in 70% and 80% yields, respectively, by Sonogashira coupling between 4-ethynyl-*N*,*N*-dimethylaniline and mono- or dibromocorannulene, respectively, at elevated temperatures (Scheme 1). Tetrakis[4-(dimethylamino)phenylethynyl]corannulene **3** was synthesized by Stille cross-coupling, which proceeded with 80% yield, from the corresponding tetrabromocorannulene. For the Stille reaction with the less reactive pentachlorocorannulene precursor, a sterically demanding nucleophilic *N*-heterocyclic carbene[6c,14] was employed as the ligand for Pd(0), and penta-substituted compound **4** was obtained in 30%

dx.doi.org/10.1021/jo302217n | J. Org. Chem. 2012, 77, 11014−11026

Scheme 1. Syntheses of Corannulene Derivatives 1−8[a]

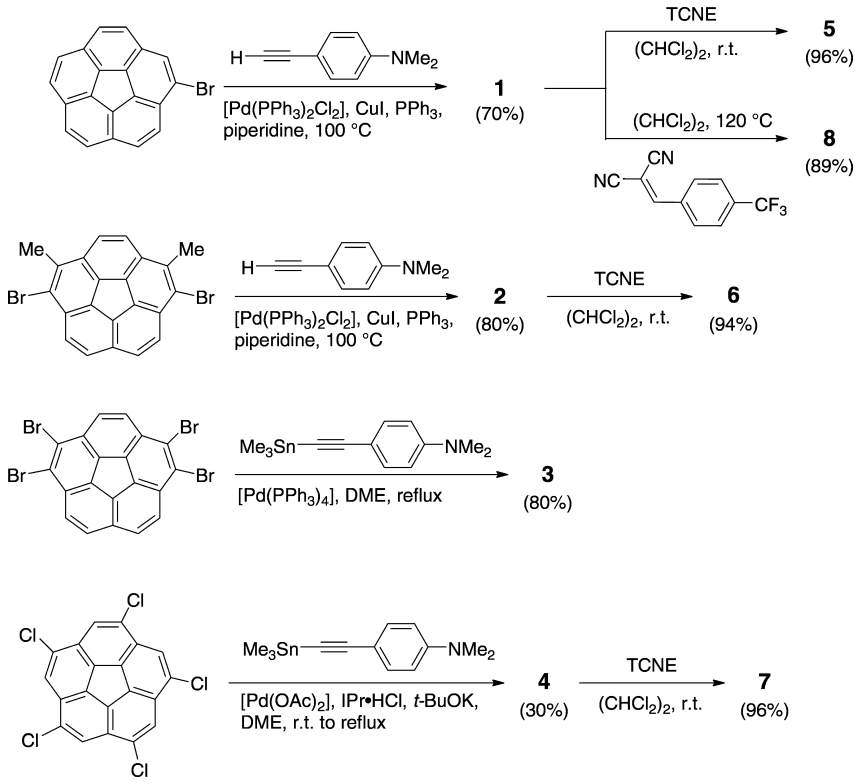

[a]TCNE = tetracyanoethene, DME = 1,2-dimethoxyethane, and IPr = 1,3-bis(2,6-diisopropylphenyl)imidazol-2-ylidene.

yield. The first-order patterns of the ^{1}H NMR and ^{13}C NMR spectra ($CDCl_3$, 298 K) of **2**−**4** indicate signal degeneracy consistent with C_{2v}, C_{2v}, and C_{5h} symmetries, respectively, in solution.

The CA−RE reactions between the donor-activated acetylenes (**1**, **2**, and **4**) and TCNE were conducted with an excess amount of TCNE (1.5 equiv per ethynyl functionality) at room temperature in 1,1,2,2-tetrachloroethane to afford the corresponding 1,1,4,4-tetracyanobuta-1,3-dienyl- (TCBD) substituted corannulenes **5**−**7** in excellent yields (94−96%). To facilitate the stereochemical analysis of butadiene-substituted corannulenes by NMR, 2-[4-(trifluoromethyl)benzylidene]malononitrile[15] was allowed to react with **1** at 120 °C for 2 d. (*E*)-Configured butadiene **8** was isolated in 89% as the only product due to the high torquoselectivity of this reaction.[8d,e,15b]

The analogous reaction of **3** and TCNE did not reach completion, even with a large excess of TCNE at elevated temperature (120 °C) and reaction times of more than a week. Only molecules having molecular composition of [**3** + 2 TCNE] were detected by mass spectrometry.[16] Prolonged reaction time resulted in decomposition of these intermediate species. The sluggish reactivity of aromatic *o*-diacetylenes has been noticed previously by Tobe and co-workers[17] and our group,[8a] possibly resulting from the electron-withdrawing power of the TCBD moiety formed in the first addition step and from steric hindrance by this bulky *ortho* substituent.

Structural Features of Monocyanobutadienyl Corannulenes 5 and 8. The ^{1}H NMR spectra for singly TCBD-functionalized **5** (500 MHz, CD_2Cl_2) showed concentration-dependent behavior. At high concentrations, the ^{1}H resonances from the $N(CH_3)_2$ group and the aromatic protons *ortho* to the $N(CH_3)_2$ group shifted upfield ($\delta(N(CH_3)_2)$ = 3.142 ppm at 0.77 mM and 3.113 ppm at 76.7 mM), whereas the doublet at ca. 8.10 ppm and the singlet at ca. 7.95 ppm from the corannulene unit shifted downfield (Figure 1). At high concentration (76.7 mM), some of the corannulene protons in **5** exhibited NOE enhancements by irradiation at the $N(CH_3)_2$ frequency (Figure 2); in contrast, such a phenomenon was not observed in the dilute solution (7.7 mM), even after an acquisition time increased by a factor of 10. Similarly, the $N(CH_3)_2$ signal of the other singly functionalized corannulene **8** exhibited an upfield shift upon concentration: $\delta(N(CH_3)_2)$ = 2.863 ppm at 2.14 mM and 2.835 ppm at 36.2 mM (see the Supporting Information). The similar concentration dependency for **5** and **8** suggested weak intermolecular association, where $N(CH_3)_2$ groups are situated in a shielding environment close to a corannulene unit, as indicated by the upfield shifts of these signals and the NOE results.

Compound **8** crystallizes in the triclinic space group $P\bar{1}$ with two molecules of **8** and two $CHCl_3$ in the asymmetric unit; the symmetry-independent molecules are essentially superimposable. Four CF_3 groups cluster around an inversion center, forming a fluorine-rich region, and the two molecules of **8** arrange in a dimeric fashion, both related by the center of inversion (Figure 3a). In each dimeric entity, the *N*-methyl group of one molecule is embedded by the concave surface of the corannulene unit of the symmetry-related molecule (shortest C_{NMe2}-to-$C_{corannulene}$ distance = 3.33 Å) and is proximal to the aniline ring of the latter.[18] Such a dimeric structure, were it to persist at higher solution concentrations, could explain the shielding and NOE enhancement observed in the variable concentration NMR spectra.

The butadiene torsion angles are ∼63° for **8**. In a related compound **9**, where a phenyl ring replaces the corannulene unit of **8**, the analogous torsion angle is 67° (Figure 3b);[15b] in TCBD molecule **10** (2,3-bis[4-(dimethylamino)phenyl]buta-1,3-diene-1,1,4,4-tetracarbonitrile), related to **5**, the corresponding torsion of 62° was found (Figure 3c).[8a] This similarity supports the idea

dx.doi.org/10.1021/jo302217n | J. Org. Chem. 2012, 77, 11014−11026

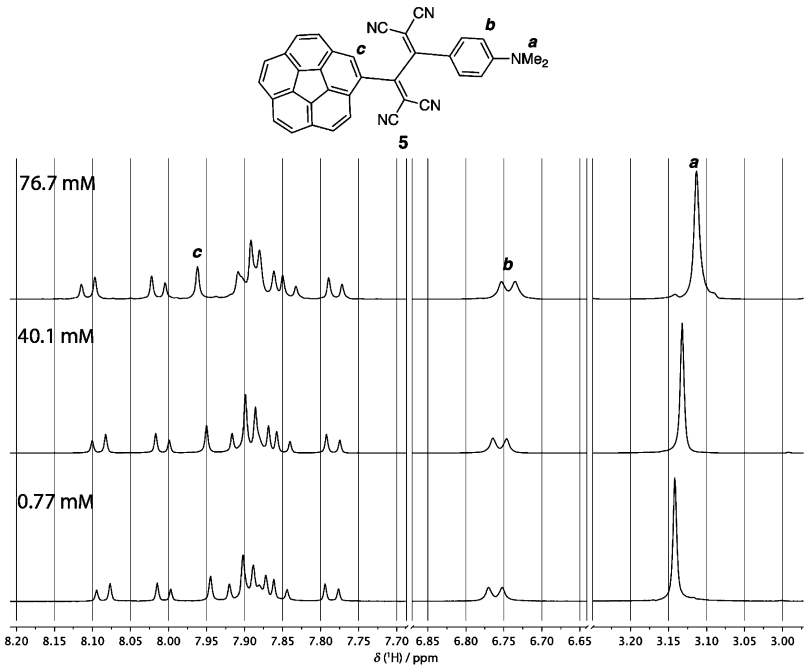

Figure 1. Partial ^{1}H NMR spectra (500 MHz, CD_2Cl_2, 293 K) of **5** at concentrations indicated at the upper left corner of each trace. Signal assignments are given.

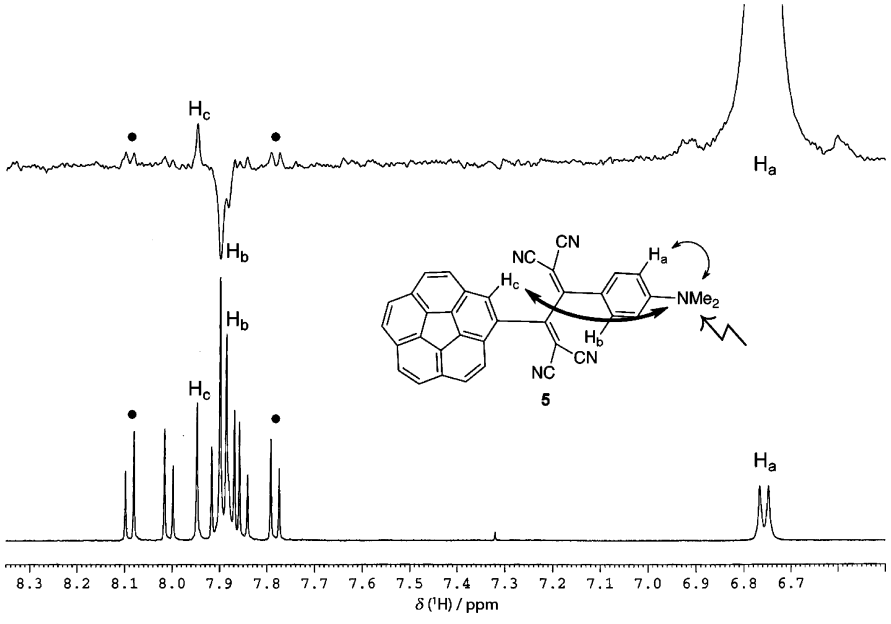

Figure 2. Upper trace: partial ^{1}H 1D-NOE difference spectrum (500 MHz, 293 K) of **5** (76.7 mM in CD_2Cl_2), obtained by irradiation at the NMe_2 resonance. Lower trace: the corresponding ^{1}H NMR spectrum for comparison. Signal assignments are given; solid circles indicate two doublets from corannulene protons.

that the skew, synclinal conformation of 2,3-diarylbuta-1,3-diene is an easily accessible minimum.

The dispersion-enabled density functional, B97-D, together with the def2-TZVPP basis set was used to study the conformation of butadienyl corannulene **8**.[19,20] Two sets of low-energy conformers **8a**/**8b** and **8c**/**8d** were found; the conformer in each set is related to each other by bowl inversion of the corannulene unit, and the conformers in different sets by the rotation about the $C_{butadiene}-C_{corannulene}$ single bond (Table 1). The *N*,*N*-dimethylanilino groups situate at the convex face of the corannulene bowl for the higher energy **8a** and **8c** and at the concave side for the more stable bowl-inversion isomers **8b** and **8d**; the geometry of the lowest energy **8d** resembles the conformation seen in the X-ray analysis. All four conformers exhibit synclinal butadiene torsion (44°−50°). Comparison between the structures of calculated **8d**, $\mathbf{8}_{dimer}$, and **8** (X-ray) suggests that the molecule can adapt the conformation readily for dimer formation, but structural changes to widen the torsion angle of the butadiene and to increase the coplanarity between the aniline and dicyanovinyl moieties are nevertheless necessary.

For $\mathbf{8}_{dimer}$, the computed ^{1}H NMR chemical shift of the $N(CH_3)_2$ group, which locates inside the corannulene bowl

dx.doi.org/10.1021/jo302217n | J. Org. Chem. 2012, 77, 11014−11026

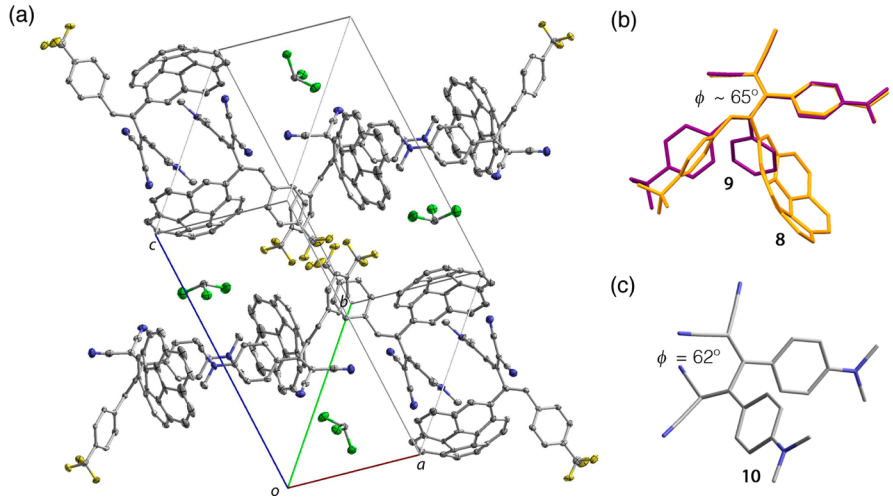

Figure 3. (a) ORTEP representation of compound **8** with thermal ellipsoids shown at the 40% probability level, 100 K. Color code: gray = C, blue = N, yellow = F, and green = Cl. Hydrogen atoms are omitted for clarity. (b) Overlay of **8** (orange, torsion angle $\phi = 63°$) and **9**, a phenyl analog of **8** (purple, $\phi = 67°$).[15b] (c) Structure of 2,3-bis[4-(dimethylamino)phenyl]buta-1,3-diene-1,1,4,4-tetracarbonitrile (**10**); torsion angle about the butadiene unit $\phi = 62°$.[8a]

Table 1. Geometric, Energetic, and NMR Parameters of 8, Calculated at the B97-D/def2-TZVPP Level of Theory in the Gas Phase

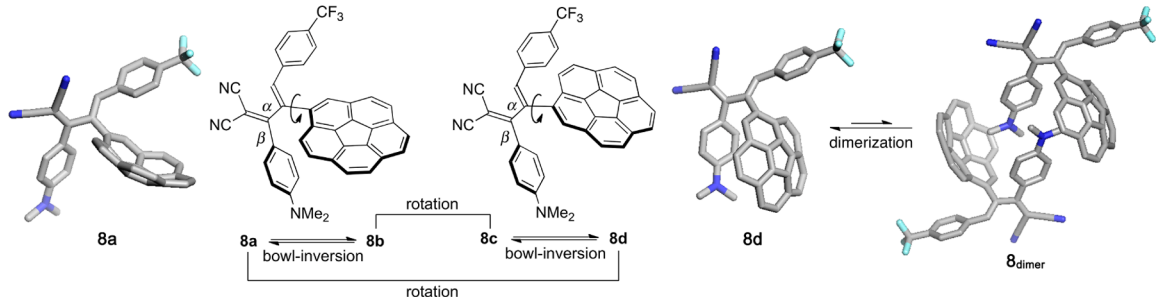

	8a	8b	8c	8d	8_{dimer}	8 (X-ray)
location of aniline relative to corannulene	convex	concave	convex	concave	concave	concave
relative energy E_0(kcal/mol)[a]	1.00	0.24	0.87	0.00	−26.8[e]	
butadiene torsion α (deg)[b]	45.7	43.7	49.7	44.3	57.7	63.1
aniline−vinyl torsion β (deg)[b]	35.2	46.0	32.2	44.4	25.3	30.3
$N(CH_3)_2$ chemical shift (ppm)[c]	2.92	1.69	2.97	1.61	−2.19	
CF_3 chemical shift (ppm)[d]	−87.40	−86.99	−87.34	−87.07	−87.19	
bowl depth (Å)	0.93	0.93	0.93	0.93	0.92	0.88
inversion barrier (kcal/mol)	11.13	11.90	10.38	11.25		10.2, 10.8

[a]Zero-point corrected energy, relative to **8d**. [b]Absolute values are given. [c]CSGT calculations, relative to $Si(CH_3)_4$. [d]CSGT calculations, relative to $CFCl_3$. [e]ZPE (zero-point energy)-uncorrected, calculated as $E(\mathbf{8}_{dimer}) - 2 \times E(\mathbf{8d})$; value in CH_2Cl_2: −24.8 kcal/mol. See the Supporting Information for DFT estimations at other levels of theory.

region, appears at −2.19 ppm (Table 1). This result is qualitatively in line with the upfield shifts of the $N(CH_3)_2$ resonance for **5** and **8** noticed in the more concentrated solutions (vide supra), suggesting that a similar kind of intermolecular association happens in solutions. However, the strength of this interaction is weak as indicated by the minor change in ^1H chemical shifts found experimentally. The calculated dimerization energy in solution ($E(\mathbf{8}_{dimer}) - 2E(\mathbf{8d})$, negative value implies dimer more stable) at best places extreme limits on the actual dimerization energy. When using DFT-D in a continuum solvent method like COSMO, dispersion of the explicit molecules is included but not for the solvation shell. When using DFT without dispersion then neither the explicit molecules nor the solvent contribute any dispersive component. The former tends to strongly overestimate the binding, whereas the latter is more likely to underestimate the value. With a range of ca. −24.8 kcal/mol for DFT-D/COSMO ($B97\text{-}D/def2\text{-}TZVPP,CH_2Cl_2//B97\text{-}D/def2\text{-}TZVPP$) down to ca. +1.72 kcal/mol for DFT/COSMO ($B3LYP/def2\text{-}TZVPP,CH_2Cl_2//B97\text{-}D/def2\text{-}TZVPP$), one has a wide berth to fill with interpretation (Table 1 and Supporting Information). Certainly, a light tendency for **8** to dimerize remains consistent with the NMR shifts observed, the X-ray structure, and the computational model.

Corannulene undergoes a rapid bowl-to-bowl inversion process at room temperature, with an estimated barrier of 11.5 kcal/mol.[3a,13a] Some monosubstituted corannulenes display barriers to bowl inversion of 10.2−11.3 kcal/mol when studied by variable-temperature NMR (VT-NMR).[2a] The trifluoromethylphenyl derivative **8** displays two sets of NMR signals with unequal intensities below $T_c = 220$ K; reversible (de)coalescence indicates an equilibrium structural interconversion (Figure 4). At 183 K, the more stable conformer shows $N(CH_3)_2$ NMR

dx.doi.org/10.1021/jo302217n | J. Org. Chem. 2012, 77, 11014−11026

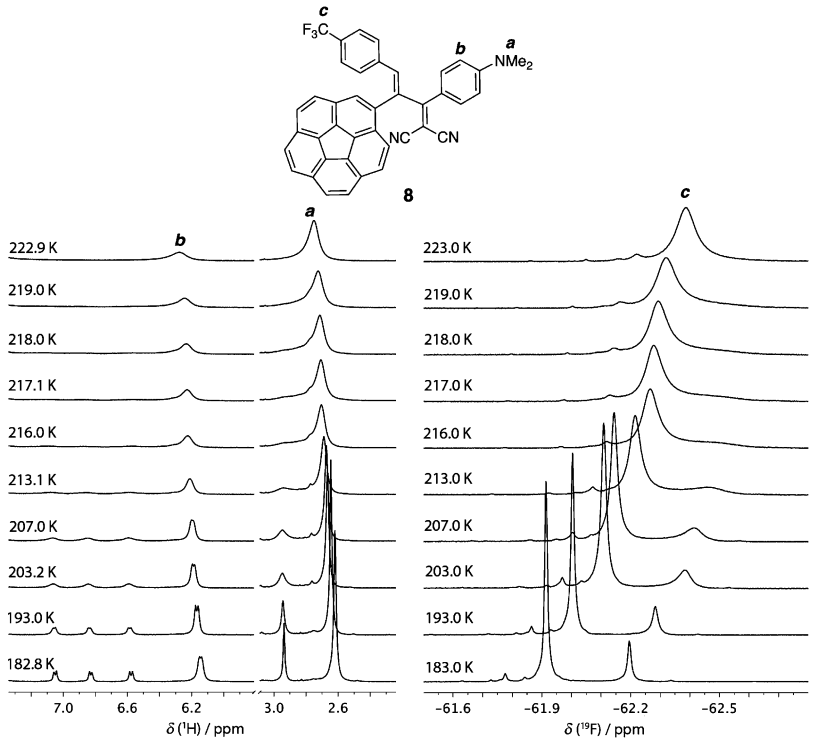

Figure 4. Partial ^{1}H (500 MHz, CD_2Cl_2, left) and ^{19}F VT-NMR (470 MHz, CD_2Cl_2, right) spectra of **8**. The temperature at which each trace was recorded is shown on the left. Signal assignments are given.

resonance at upper field (2.62 vs 2.94 ppm) and CF_3 at lower field (−61.92 vs −62.19 ppm) relative to the less stable conformer. The unequal intensity suggested two structures of different energy ($\Delta G \sim 0.65$ kcal/mol at T_c), most likely two diastereoisomers related by bowl inversion. The assignment is supported by the calculated upfield $N(CH_3)_2$ chemical shifts and downfield CF_3 shifts for the more stable conformers **8b** and **8d**, relative to those for **8a** and **8c**, respectively (Table 1). Bowl-inversion barriers of $\Delta G^{\ddagger} = 10.2$ kcal/mol (minor to major) and 10.8 kcal/mol (major to minor) were estimated at the coalescence temperature $T_c = 220$ K by the Gutowsky−Holm approximation and the Shanan-Atidi−Bar-Eli method.[21] B97-D/def2-TZVPP energies E_0 (Table 1) correlate well with both the bowl-inversion barrier and the relative energy of the two bowl-inversion forms. For **5**, the two bowl-inversion isomers appear to have similar energies; the inversion barrier was estimated to be $\Delta G^{\ddagger} = 10.2$ kcal/mol at $T_c = 205$ K (Supporting Information).

Conformation of Multiply Cyanobutadienyl-Functionalized Corannulenes 6 and 7. As previously mentioned, multiply functionalized corannulenes **2** and **4** display NMR spectra consistent with C_{2v} and C_{5h} symmetry at room temperature, respectively; however, these symmetry characteristics do not persist in the corresponding bis- and pentakis-TCBD compounds **6** and **7**, as a result of substantial intersubstituent interactions. VT-NMR experiments permitted the characterization of these interactions and their interplay with the curved structure of corannulene in **6** and **7**. The presence of multiple low-symmetric diastereoisomers at low temperatures, however, hampered the analysis of bowl-inversion processes associated with these electron-deficient corannulenes.

For pentakis-TCBD **7** at temperatures lower than 300 K, multiple magnetically distinct *N*-methyl groups were observed and the same holds true for its aromatic protons *ortho* to the amino group (Figure 5). Cooperative contributions from the synclinal conformation of TCBD and the curvature of corannulene result in some of the five peripheral substituents being positioned at one face. The situation is even more complicated when there are two and three substituents at either face of the corannulene, since these two substituents can have 1,3-, 1,5-, or 1,7-relationships, each resulting in C_1 symmetry, the subgroup of C_{5h}. Despite this complexity, the ^{1}H NMR signals from the corannulene moiety are perceptibly sharper than those from the aniline units at the same temperature range. At temperatures above 363 K, the increased rate of interconversion of one C_1 conformer into another restores the "expected" C_5 symmetry of **7**.

Reducing the number of aniline-TCBD substituents from five to two reduces the number of possible conformers. For bis-TCBD **6**, the ^{1}H NMR spectra display two singlets around 8.05 ppm, two doublets around 7.85 ppm, and another two doublets around 7.70 ppm (temperature = 273 ± 30 K) in the region where ^{1}H signals of corannulene are expected, and these two sets of signals have roughly equal intensities (Figure 6b). According to the molecular structure of **6**, the two sets of ^{1}H signals were assigned to two magnetically distinct, 2-fold symmetric isomers in solution.

One of these 2-fold symmetric molecules has the two TCBD arms pointing toward the same face of its corannulene unit (*syn*-**6**), and the other one has TCBDs at opposite faces (*anti*-**6**) (Scheme 2). The comparable NMR intensities of *syn*-**6** and *anti*-**6** are reminiscent of the similar populations of the bowl-inversion pair of mono-TCBD **5**. The coexistence of both isomers suggests restricted rotation about the $C_{butadiene}-C_{corannulene}$ single bond due to the impedance of the *o*-methyl groups. The strong interaction observed between these neighboring functionalities testifies to the blocked reactivity of tetraacetylene **3** toward the addition of the third and fourth equivalents of TCNE (vide supra). At sufficiently high temperature, a single species with a time-averaged 2-fold symmetry

dx.doi.org/10.1021/jo302217n | J. Org. Chem. 2012, 77, 11014−11026

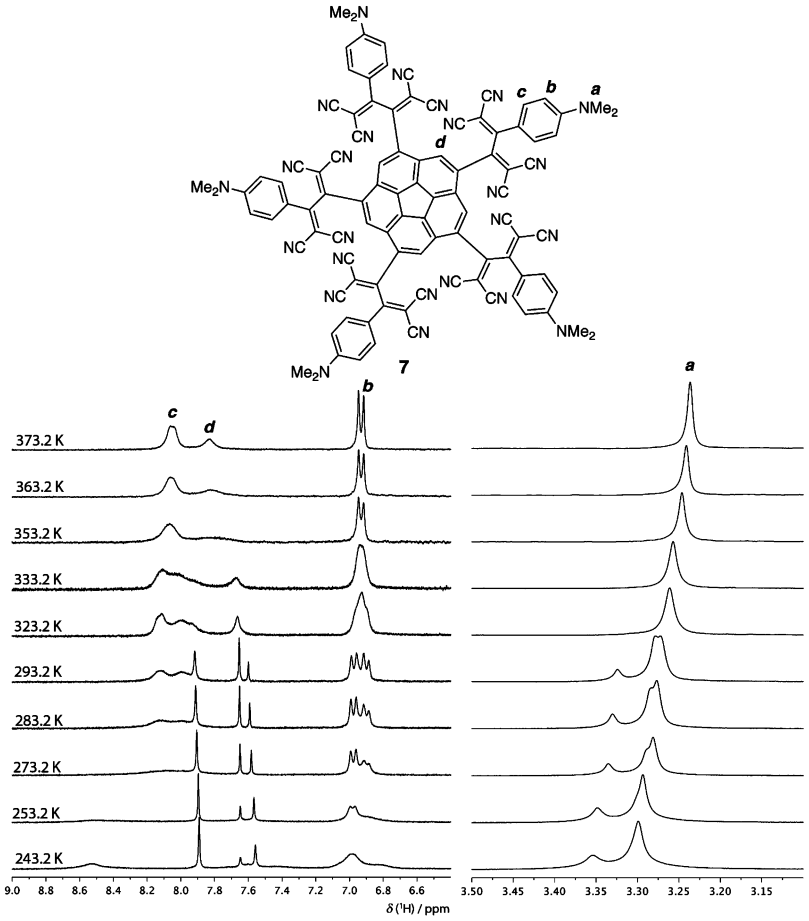

Figure 5. Partial ^{1}H VT-NMR spectra (300 MHz, $(CDCl_2)_2$) of **7**. Temperature at which each trace was recorded is shown on the left. Signal assignments are given.

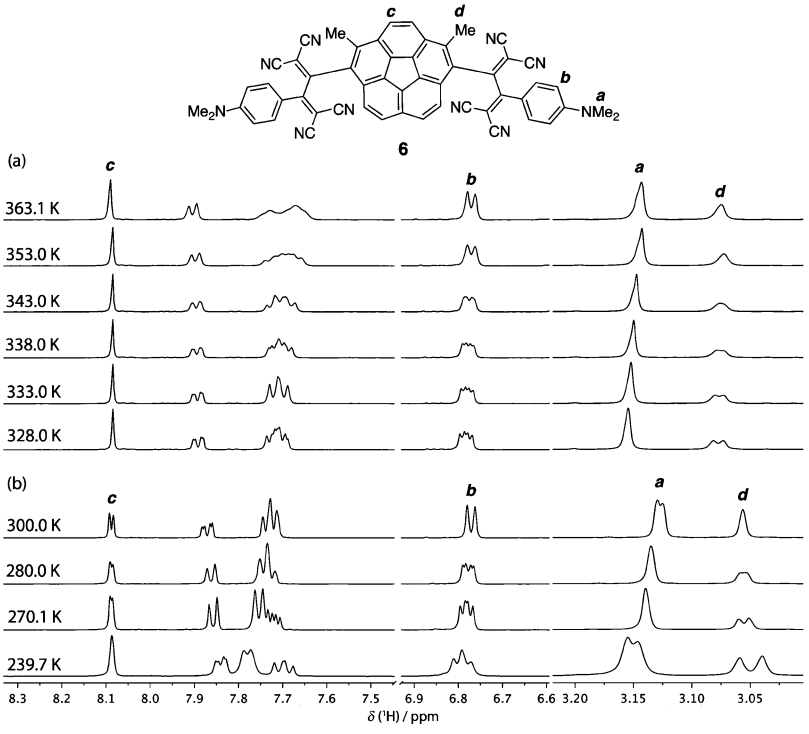

Figure 6. Partial ^{1}H VT-NMR spectra (500 MHz) of **6** (a) in $(CDCl_2)_2$ at 328−363 K and (b) in CD_2Cl_2 at 240−300 K. Temperature at which each trace was recorded is shown on the left. Signal assignments are given.

dx.doi.org/10.1021/jo302217n | J. Org. Chem. 2012, 77, 11014−11026

Scheme 2. Graphic Representation of Various Conformers of 6

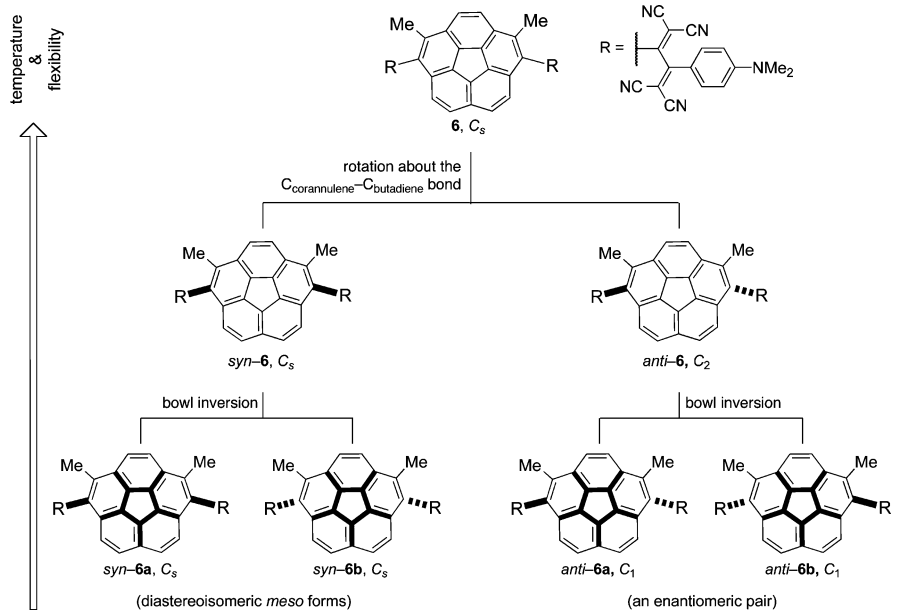

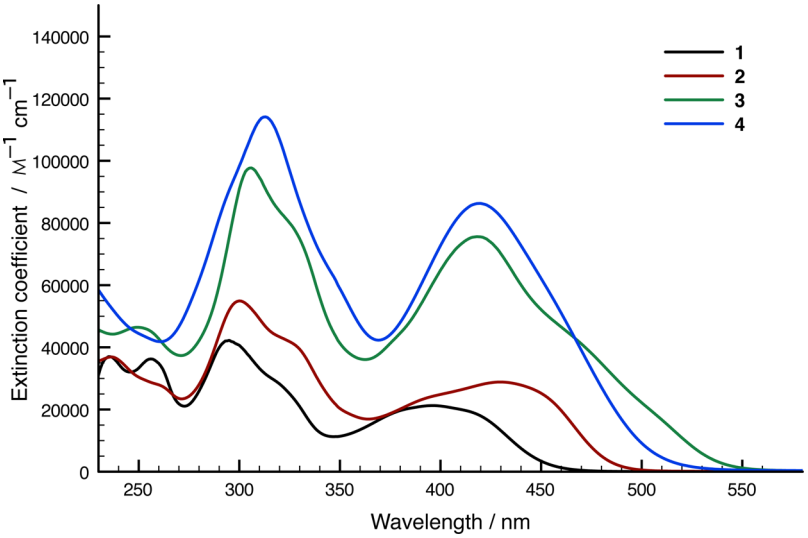

Figure 7. UV/vis absorption spectra of **1**–**4** in CH_2Cl_2 at 298 K ($c \sim 10^{-5}$ M).

was observed by NMR (Figure 6a); a barrier of 19.2 kcal/mol at T_c = 343 K for this restricted rotation was estimated. Atropisomerism with a similar barrier had been previously observed for a TCBD–C_{60} conjugate, in which the rotation about the bond connecting the two moieties was also hindered by a neighboring methyl group attached to the carbon sphere.[22]

It should be noted that the above stereochemical analysis for **6** provides a simplified picture and is only applicable at high temperatures where the corannulene core is inverting rapidly and can be considered as a time-averaged planar structure. Taking the curvature of this core unit into consideration results in four conformers, *syn*-**6a**, *syn*-**6b**, *anti*-**6a**, and *anti*-**6b**; the former two are both C_s symmetric molecules, and the latter two are C_1 symmetric and form a pair of enantiomers (Scheme 2). At lower temperatures, the bowl-inversion motion slows, and three magnetically distinct species can be observed and, in principle, examined with regard to their bowl-inversion dynamics; however, complicated and unresolvable ^{1}H NMR signals were recorded, making interpretations about the molecular conformation in this temperature range difficult (down to 150 K in Freon ($CDCl_2F$) or down to 200 K in CD_2Cl_2). The syn-/anticlinal conformational equilibrium of the butadiene moieties may be one of the sources to complicate the analysis. The barrier of this process is expected to be higher than that of 2,3-diphenylbuta-1,3-diene (ca. 5 kcal/mol by MP2/6-311++G**),[9b] caused by the neighboring methyl substituent.

Electronic Absorption and Emission Spectra. Two absorption bands in the region of 280–350 and 350–550 nm were observed for **1**–**4** in dichloromethane (Figure 7). The broad, long-wavelength absorptions in the latter region are assigned to have intramolecular charge-transfer (ICT) character as they diminished when these solutions were treated with trifluoroacetic acid (TFA); the resulting spectra closely resemble those of phenylethynyl corannulenes.[6c] This observation also suggested that the absorptions in the higher energy region (280–350 nm) are mostly due to the π–π^* transitions of ethynylcorannulenes. The optical gaps (ΔE_{opt}) estimated from the absorption onset (**1**: 2.44, **2**: 2.39, **3**: 2.18, and **4**: 2.30 eV)

dx.doi.org/10.1021/jo302217n | J. Org. Chem. 2012, 77, 11014–11026

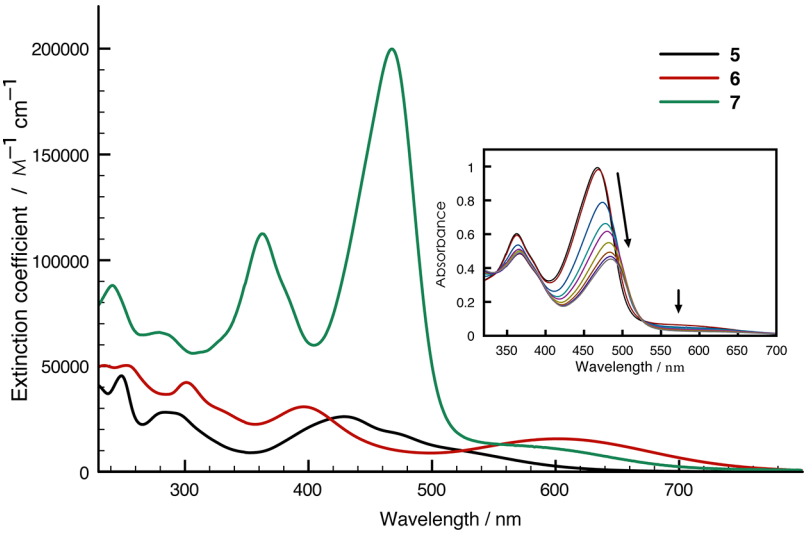

Figure 8. UV/vis absorption spectra of **5**–**7** in CH_2Cl_2 at 298 K ($c \sim 10^{-5}$ M). Inset shows the changes of absorption spectra of **7** upon addition of trifluoroacetic acid (up to 10^5 equiv).

decrease, by and large, as the number of electron-donating group increases. Excitation energies (ΔE_{calc}, to the first allowed excited state) calculated at the level of TD B97-D/def2-TZVPP show the same trend (**1**: 2.22, **2**: 2.08, **3**: 1.75, and **4**: 2.00 eV in the gas phase, and **1**: 2.07, **2**: 1.89, **3**: 1.59, and **4**: 1.76 eV in CH_2Cl_2), but are systematically underestimated relative to the experimental values.

The larger optical gap of **4** compared to that of **3** signifies that the exact positioning of the substituents and thus the molecular symmetry substantially influences the electronic structure of corannulene derivatives. On the time scale of the UV/vis experiment, the bowl-inversion of **1**–**3** should be frozen and the spectra should arise from molecular symmetries C_1 or C_s. Hence, there should be nondegenerate A-type orbitals for **1** or A′- and A″-type orbitals for **2** and **3**. In the case of **4**, the C_5 symmetry results in sets of closely separated degenerate E_1- and E_2-type orbitals.[6c] The observation of similar electronic absorption behavior between di- and penta-substituted compounds **2** and **4** as compared to **3** and **4** reflects a "redistribution" of orbital energies by high molecular symmetry. According to the TD-DFT calculations, the first two transitions of **4** are essentially forbidden (oscillator strengths $f = 0.00$); the first allowed transition ($S_3 \leftarrow S_0$) requires 1.76 eV for excitation, which is close to the value predicted for **2** (1.89 eV).

Similar to their trimethylsilyl, phenyl, alkylphenyl, and alkoxyphenyl analogues, anilino compounds **1**–**4** show strong photoluminescence in solution.[6c] Compared to the parent corannulene (λ_{em} = 423 nm, Φ_f = 0.03), multivalent phenylethynylcorannulenes ($\lambda_{em} \sim$ 500 nm), and multivalent 3,4,5-trialkoxyphenylethynylcorannulenes ($\lambda_{em} \sim$ 530 nm), introduction of aniline groups induces a bathochromic shift of the emission bands to ca. 600 nm. In the present series, emission at λ_{em} = 533 nm (Φ_f = 0.98) for **1**, λ_{em} = 538 nm (Φ_f = 0.93) for **2**, λ_{em} = 593 nm (Φ_f = 0.76) for **3**, and λ_{em} = 595 nm (Φ_f = 0.56) for **4** was observed (see the Supporting Information for spectra). While many push–pull chromophores experience the rapid radiationless decay from their twisted or distorted ICT excited states,[23] the inclusion of cylindrically symmetric acetylene units in peripherally functionalized corannulenes on the one hand keeps molecular rigidity for radiative relaxation, and on the other hand allows for the free choice of functionality around the corannulene core. Thus, fluorescence compounds with blue, green, and orange colors could be obtained with reasonable emission quantum yields.

The cyanobutadiene molecules **5**–**7** exhibit red-shifted absorption bands compared to their ethynyl precursors (Figure 8). For **5**, the high-energy absorption at 248 nm is attributed to the local excitation of the aniline and the corannulene groups, the 260–350 nm band originates from the 2,3-diaryl TCBD system, and the broad and multiband absorption covering 350–700 nm is dominated by ICT character. In the case of **6**, the two higher-energy transitions present in **5** were similarly observed; however, two well-separated ICT absorptions at 396 and 600 nm were recorded. A similar two-band ICT absorption at 384 and 532 nm was observed in an analogous compound where a 2,2′-diethoxy-1,1′-binaphthalene-3,3′-diyl unit is used in place of the 2,4-dimethyl-corannulen-1,6-diyl unit of **6**.[24] The similarity between the latter two molecules, in comparison to **5**, indicates the critical steric and electronic effects of the *ortho*-dimethyl or *ortho*-diethoxy groups on modifying HOMO/LUMO manifolds.

For **7**, two very intense absorptions at 363 nm (ε 112 500 M^{-1} cm^{-1}) and 468 nm (ε 199 800 M^{-1} cm^{-1}) were observed, with one weak shoulder around 600 nm (Figure 8). As discussed earlier, the C_5 symmetry of its precursor **4** was removed by the steric interactions between TCBD moieties. Thus, the exceptionally high molar absorption of **7** is likely due to the presence of five push–pull chromophoric units in a single molecule. Even though the nature of the absorption at 363 nm remains unclear, the appearance of a strong band at 468 nm together with a shoulder at 600 nm (nonvanishing until ca. 800 nm) is characteristic of crowded TCBD molecules having a strong electron-withdrawing unit at the 2-position of the butadiene. For instance, dialkylanilino-substituted octacyano[4]dendralenes display absorptions around 490 nm with shoulders at 650 nm for,[25] and strong absorptions around 465 nm with shoulders at 600 nm for, multivalent TCBDs.[8a]

As mentioned earlier, the ICT absorptions of push–pull chromophores are diminished by TFA protonation (pK_a 0.52 in H_2O) of the electron-donating aniline functionality (for $PhNMe_2H^+$, pK_a 5.07 in H_2O).[26] Larger amounts of TFA are generally needed to fully quench the ICT bands of **5** and **6** as compared to **1**–**4** becase of the reduced basicity of the anilino groups induced by the presence of electron-withdrawing cyanovinyl moieties. However, the complete disappearance of the ICT absorptions of **7** upon treatment with TFA was not observed (Figure 8 inset). The intensities of the ICT absorptions at 363 and 468 nm were reduced, but a saturation of

dx.doi.org/10.1021/jo302217n | J. Org. Chem. 2012, 77, 11014–11026

spectral change was reached even after the employment of 10^5 equiv of TFA. The difficulty in achieving global protonation reflects the combined and strong electron-withdrawing power of five cyanovinyl groups and of protonated aniline groups. Moreover, it further underscores the proximity between aniline substituents caused by the curvature of corannulene and the geometrical preferences of 2,3-diaryl butadienes; global protonation would otherwise produce strong and unfavorable Coloumbic repulsions.

Electrochemistry of Conjugates 1−7. Investigations of **1**−**7** and *sym*-pentakis(trimethylsilylethynyl)corannulene **11**[6c] were carried out by cyclic voltammetry (CV) and rotating disk voltammetry (RDV) in CH_2Cl_2 (+ 0.1 M *n*-Bu_4NPF_6); potentials reported in Table 2 are referenced to the ferricinium/ferrocene couple (Fc^+/Fc). For some derivatives, reproducible data could only be observed on freshly polished working electrodes due to electrode inhibition during redox processes.

Table 2. Cyclic Voltammetry (CV; scan rate ν = 0.1 V s^{-1}) and Rotating Disk Voltammetry (RDV) Data in CH_2Cl_2 (+ 0.1 M *n*-Bu_4NPF_6)[a]

	CV			RDV	
compd	$E°$/V[b]	ΔE_p/mV[c]	E_p/V[d]	$E_{1/2}$/V[e]	slope/mV[f]
11	−1.81	70		−1.81 (1e$^-$)	60
	[g]			−2.18 (1e$^-$)	60
1			+0.37	+0.37 (1e$^-$)	50
			−2.13	−2.25 (1e$^-$)	70
2			+0.44	[h]	
			+0.35		
	−1.86	60		−1.86 (1e$^-$)	60
3			+0.20	[h]	
	−1.92	60		−1.93 (1e$^-$)	60
			−2.35	−2.29	
4			+0.42	[h]	
			+0.33		
	−1.90	60		−1.86	60
5	+0.91	70		+0.94 (1e$^-$)	60
	−0.83	90		−0.85 (1e$^-$)	70
	−1.18	80		−1.23 (1e$^-$)	75
6			+0.92[i]	+0.90 (2e$^-$)	[i]
	−0.71	120		−0.73 (2e$^-$)	100
	−1.24	150		−1.36 (2e$^-$)	150
7			+0.95		
	−0.72[j]			−0.72 (2e$^-$)	
	−0.80[j]			−0.82 (1e$^-$)	
	−0.90[j]			−0.90 (1e$^-$)	
	−1.03[j]			−1.05 (1e$^-$)	
	−1.31[j]				
	−1.41[j]			−1.45 (5e$^-$)	200
	−1.52[j]				
	−1.64[j]				
	−1.86[j]				

[a]All potentials are given vs the Fc^+/Fc couple used as the internal standard. [b]$E° = (E_{pc} + E_{pa})/2$, where E_{pc} and E_{pa} correspond to the cathodic and anodic peak potentials, respectively. [c]$\Delta E_p = E_{pa} - E_{pc}$. [d]$E_p$ = irreversible peak potential. [e]$E_{1/2}$ = half-wave potential. [f]Logarithmic analysis of the wave obtained by plotting E vs $\log[I/(I_{lim}-I)]$. [g]A second reversible electron transfer is observed at −2.20 V for scan rates higher than 1 V/s. [h]Electrode inhibition during oxidation. [i]Electrode inhibition during oxidation; on the reverse scan in CV, a redissolution peak is observed at +0.83 V. [j]These potentials were determined from the cyclic voltammetry convolution.

The parent corannulene is known to undergo up to four reduction steps at rather negative potentials, and these potentials are strongly dependent on the choice of solvents and supporting electrolytes, especially for the latter three reductions.[27] The first two reductions occur at roughly $E_{1/2}$ −2.35 and −3.02 V versus Fc^+/Fc.[28] Such processes are made more favorable by the electron-withdrawing acetylenic substituents in **11** (−1.81 and −2.18 V). In the case of **1**−**4**, the end-capped aniline groups counteract the effects of lowering reduction potentials by $C_{sp}{\equiv}C_{sp}$ units; there is no clear correlation between the first reduction potentials and the number of ethynyl substituents: $E_{1/2,red}$: **2** (−1.86) ≈ **4** (−1.86) > **3** (−1.93) > **1** (−2.25 V). The absence of a second reduction for more easily reduced compounds **2** and **4** suggests relatively large potential gaps between the first and the second reductions as compared to **3**, **11**, and corannulene.

On the oxidation side, strong electrode inhibition was often observed, and a nonmonotonic trend was again observed: $E_{p,ox}$: **1** (+0.37) > **2** (+0.35) > **4** (+0.33) > **3** (+0.20 V). Clearly, the *ortho* 4-(*N*,*N*-dimethylaminophenyl)ethynyl groups in **3** together greatly amplify the electron donating in the molecule; moreover, the oxidation potential of **3** is lower than those of 4,4′-(buta-1,3-diyne-1,4-diyl)bis(*N*,*N*-dialkylanilines), which exhibit oxidation potentials in the range of +0.26 − +0.32 V.[25] The observation of a second oxidation event (at ca. +0.43 V) for **2** and **4** indicates that the anilino substituents are not independent redox sites; electronic communication is effective even through the fairly large π-framework of ethynylcorannulene.

For TCBDs **5**−**7**, the oxidation of aniline is shifted to more positive potentials by more than 500 mV due to the presence of cyanovinyl functionalities, which is in agreement with our previous studies.[25] Contrasting with the oxidation behaviors of **2** and **4**, the oxidations of **6** and **7** show only one anodic peak whose characteristics correspond to the oxidation of two (for **6**) or five (for **7**) independent anilino centers. Deposition occurs for **6** during oxidation, which gave a sharp redissolution peak at +0.83 V during the reverse scan.

First reductions for **5**−**7** were recorded around −0.71 to −0.83 V; compounds with higher numbers of cyanovinyl functionalities are more easily reduced, as one would expect. However, this effect is marginal going from **6** to **7**. Two, well-defined, and reversible reductions on the TCBD moieties were observed for **5** at any scan rate, while similar but broad reductions were observed in the case of **6**. From the peak shapes and especially from the peak potential differences, it is clear that, for **6**, each step corresponds to two overlapping reversible one-electron transfers separated by about 50 mV for the first reduction and by 75 mV for the second step. This small, but noticeable peak separation is suggestive of interactions between the two TCBD moieties.

For highly functionalized **7**, the CV was reproducible, but a series of unresolved redox processes occurs on the reduction side. Convolution of the experimental curves suggests two sets of five reversible one-electron transfers (Supporting Information). In addition to orbital interactions through the π-system of corannulene (cf. the oxidation of **2** and **4**), the close proximity of the TCBD moieties allows for electrostatic interactions between the reduced TCBDs, and explains the observed splitting of redox potentials for the latter compounds. It should be mentioned that for **7**, the amplitude of the latter reduction peaks in CV became smaller and smaller, probably due to the decreasing solubility of the multianionic species. However, by RDV, the unresolved wave amplitudes (limiting currents) show similar amplitudes, denoting that the same number of electrons have been exchanged.

dx.doi.org/10.1021/jo302217n | J. Org. Chem. 2012, 77, 11014−11026

CONCLUSION

Peripherally functionalized corannulenes with one, two, four, and five electron-donating and/or electron-withdrawing substituents were efficiently synthesized. Their electronic absorption spectra were dominated by ICT absorptions in the visible region of 350−800 nm. Ethynylanilines **1**−**4** exhibit strong fluorescence in green or orange colors, whereas rapid and nonradiative decay might result from the ICT states for **5**−**7**. Their redox behaviors were characterized; significantly reduced and diverse reduction potentials were observed, as compared to the parent corannulene. The energy required for electronic excitation and the redox potentials were found not to alter monotonically with respect to the number of substituents. The exact positioning of the substituents, molecular symmetry, and the stability of the states formed (oxidized, reduced, or excited) all make critical contributions.

The multicyanobutadiene motifs of **5**−**8** enhance the electron-accepting power of corannulene systems, and their unique geometries were found to provoke the steric interaction between *ortho*-functionalities (for **6**), transannular steric and electrostatic interactions (for **7**), and intermolecular interactions (for **5** and **8**). Optical and electrochemical properties of functionalized corannulenes are thus subtly modified by such conformational influences, in addition to the effects from molecular symmetries and the positioning of substituents.

The adjustable absorption and fluorescence properties, curved π-surface for supramolecular interaction and metal ion stabilization/complexation, multiple reduction states, and the established and efficient methodologies for derivatization, together, make corannulenes promising candidates for electrochemically and/or photophysically active functional materials. The 1,6-diethynylcorannulene presented here is also a potential synthon for corannulene-containing polymers or cyclophane-type molecular baskets.[15b]

EXPERIMENTAL SECTION

Materials, General Methods, and Electrochemistry. See the Supporting Information.

Theoretical Calculations. The conformational analyses of the molecular systems described in this study and property calculations were carried out using the GAMESS[19] software packages at the level of B97-D/def2-TZVPP.[20] Full geometry optimizations were performed and uniquely characterized via second derivatives (Hessian) analysis to determine the number of imaginary frequencies (0 = minima; 1 = transition state). Chemical shifts were calculated by referencing the CSGT[29] isotropic magnetic shielding constants (σ) to $SiMe_4$ (σ = 31.3501 ppm, for ^1H) or to $CFCl_3$ (σ = 144.6463 ppm, for ^{19}F) in vacuum. Time dependent TD-DFT calculations in CH_2Cl_2 were performed on the optimized, gas-phase geometries.

X-ray Analysis of 8. The scattering intensity data were collected under MoK_α radiation (λ = 0.71073 Å). Cell dimensions were obtained based on 4040 reflections above 20 $\sigma(I)$ (q_{max} = 25.16°). The structure was solved by direct methods with SHELXS and refined with OLEX2 and SHELXL.[30] All non-hydrogen atoms were refined anisotropically, H-atoms isotropically with some restraints by full matrix least-squares using experimental weights $w = 1/[s^2(F_o)^2 + (0.07000\ P)^2]$, where $P = (F_o^2 + 2\ F_c^2)/3$. One corannulene moiety is partly disordered. No attempt was made to refine multiple atom positions.

Single crystals were obtained by slow diffusion of pentane into the $CHCl_3$ solution of **8** at 4 °C: $C_{41}H_{24}F_3N_2{\cdot}CHCl_3$, M_r = 753.00, crystal dimensions 0.04 × 0.11 × 0.19 mm, triclinic space group $P\bar{1}$, Z = 4, a = 11.817(2) Å, b = 14.954(2) Å, c = 20.549(3) Å, α = 70.961(5)°, β = 84.168(5)°, γ = 88.955(5)°, V = 3414.5(8) Å^3, D = 1.430 g/cm^3 at 100(2) K. Number of measured and unique reflections 39740 and 11961, respectively (R_{int} = 8.06%, R_{sig} = 12.26%). Final $R(F)$ = 6.89%, $wR(F^2)$ = 13.72% for 1119 parameters and 6279 reflections with $I > 2\sigma(I)$ (corresponding R-values based on all 11961 reflections 16.06% and 16.83%). CCDC deposition no. 901534.

*(4-N,N-Dimethylanilinoethynyl)corannulene (**1**).* A solution of bromocorannulene (280 mg, 0.856 mmol), 4-ethynyl-*N*,*N*-dimethylaniline (372 mg, 2.56 mmol), $[Pd(PPh_3)_2Cl_2]$ (30 mg, 0.04 mmol), PPh_3 (76 mg, 0.29 mmol), and CuI (50 mg, 0.26 mmol) in piperidine (15 mL) was heated at 100 °C for 1 d under N_2. Piperidine was evaporated from the cooled mixture, and the residue was subsequently passed through a small SiO_2 plug (CH_2Cl_2). The concentrated CH_2Cl_2 solution was added dropwise to hexanes; the precipitate was collected and washed one more time with hexanes to give **1** (230 mg, 70%) as a yellow solid. Mp: 165−167 °C. ^1H NMR (300 MHz, $CDCl_3$): δ = 3.02 (s, 6 H; N*Me*$_2$), 6.76 (d, J = 8.8 Hz, 2 H; *Ph*NMe$_2$), 7.63 (d, J = 8.8 Hz, 2 H; *Ph*NMe$_2$), 7.69−7.84 (m, 6 H; corannulene), 7.87 (d, J = 8.8 Hz, 1 H; corannulene), 8.02 (s, 1 H; corannulene), 8.18 ppm (d, J = 8.8 Hz, 1 H; corannulene). ^{13}C NMR (75 MHz, $CDCl_3$): δ = 40.3, 86.1, 95.1, 110.1, 112.0, 122.7, 126.4, 126.7, 127.16, 127.20, 127.3, 127.4, 127.5, 130.1, 130.7, 131.0, 131.1, 133.1, 134.9, 135.3, 135.7, 135.8, 136.2, 150.4 ppm (24 out of 27 expected peaks). IR (ATR): ν = 3024 (vw), 2893 (vw), 2804 (vw), 2185 (m), 1605 (m), 1522 (m), 1357 (w), 1228 (w), 1154 (w), 1122 (w), 1098 (w), 1064 (w), 868 (m), 827 (s), 812 cm^{-1} (s). UV/vis (CH_2Cl_2): λ_{max} (ε) = 295 (42 300), 396 nm (21 300 M^{-1} cm^{-1}). HR-ESI-MS m/z: calcd for $C_{30}H_{20}N^+$ 394.15903, found 394.15876 ([M + H]$^+$).

*1,6-Bis(4-N,N-dimethylanilinoethynyl)-2,5-dimethylcorannulene (**2**).* A solution of 1,6-dibromo-2,5-dimethylcorannulene (90 mg, 0.206 mmol), 4-ethynyl-*N*,*N*-dimethylaniline (209 mg, 1.44 mmol), $[Pd(PPh_3)_2Cl_2]$ (30 mg, 0.04 mmol), PPh_3 (76 mg, 0.29 mmol), and CuI (50 mg, 0.26 mmol) in piperidine (15 mL) was heated at 100 °C for 1 d under N_2. Piperidine was evaporated from the cooled mixture, and the residue was subsequently passed through a small plug (SiO_2; CH_2Cl_2). The concentrated CH_2Cl_2 solution was added dropwise to hexanes; the precipitate was collected and washed one more time with hexanes to give **2** (90 mg, 80%) as a yellow solid. Mp: 285−288 °C. ^1H NMR (300 MHz, $CDCl_3$): δ = 3.00 (s, 6 H; Me), 3.03 (s, 12 H; N*Me*$_2$), 6.74 (d, J = 8.8 Hz, 4 H; *Ph*NMe$_2$), 7.56 (d, J = 8.8 Hz, 4 H; *Ph*NMe$_2$), 7.81 (d, J = 8.8 Hz, 2 H; corannulene), 7.91 (s, 2 H; corannulene), 8.07 ppm (d, J = 8.8 Hz, 2 H; corannulene). ^{13}C NMR (101 MHz, $CDCl_3$): δ = 16.9, 40.3, 85.1, 99.8, 112.1, 120.4, 125.0, 126.2, 127.4, 130.5, 131.7, 132.8, 134.1, 134.3, 135.8, 138.8, 150.3 ppm (17 out of 19 expected peaks). IR (ATR): ν = 2889 (vw), 2802 (vw), 2191 (w), 1605 (s), 1519 (s), 1358 (m), 1229 (m), 1198 (m), 1064 (m), 944 (s), 815 (s), 788 cm^{-1} (s). UV/vis (CH_2Cl_2): λ_{max} (ε) = 300 (54 900), 328 (sh, 40 600), 391 (sh, 23 300), 430 nm (28 800 M^{-1} cm^{-1}); HR-ESI-MS m/z: calcd for $C_{42}H_{33}N_2^+$ 565.26383; found 565.26339 ([M + H]$^+$); calcd for $C_{42}H_{34}N_2^{2+}$ 283.13555, found 283.13509 ([M + 2H]$^{2+}$).

*1,2,5,6-Tetrakis(4-N,N-dimethylanilinoethynyl)corannulene (**3**).* $[Pd(PPh_3)_4]$ (20 mg, 0.02 mmol) was added to a solution of 1,2,5,6-tetrabromocorannulene (245 mg, 0.436 mmol) and *N*,*N*-dimethyl-4-[2-(trimethylstannyl)ethynyl]aniline (810 mg, 2.62 mmol) in anhydrous dimethoxyethane (40 mL) under N_2. The mixture was heated at reflux for 4 d. The solvent of the cooled mixture was evaporated, and the residue was passed through a small plug (SiO_2; CH_2Cl_2). The concentrated CH_2Cl_2 solution was added dropwise to hexanes; the precipitate was collected and washed one more time with hexanes to give **3** (280 mg, 80%) as a red solid. Mp: 202−204 °C. ^1H NMR (400 MHz, $CDCl_3$): δ = 3.02 (s, 24 H; N*Me*$_2$), 6.73 (d, J = 8.3 Hz, 8 H; *Ph*NMe$_2$), 7.63 (d, J = 8.2 Hz, 8 H; *Ph*NMe$_2$), 7.81 (d, J = 8.7 Hz, 2 H; corannulene), 8.07 (d, J = 8.7 Hz, 2 H; corannulene), 8.12 ppm (s, 2 H; corannulene). ^{13}C NMR (101 MHz, $CDCl_3$): δ = 40.3, 86.16, 86.24, 100.4, 100.5, 110.6, 112.0, 124.4, 124.5, 126.5, 126.8, 127.6, 131.0, 131.2, 133.1, 133.8, 134.6, 135.5, 150.3 ppm (19 out of 25 expected peaks). IR (ATR): ν = 2888 (vw), 2856 (vw), 2799 (vw), 2173 (m), 1602 (s), 1519 (s), 1442 (m), 1353 (s), 1161 (s), 944 (m), 810 cm^{-1} (s). UV/vis (CH_2Cl_2): λ_{max} (ε) = 306 (97 700), 327 (sh, 78 300), 418 (75 600), 469 nm (sh, 41 700 M^{-1} cm^{-1}). HR-ESI-MS m/z: calcd for $C_{60}H_{47}N_4^+$ 823.37952, found 823.37911 ([M + H]$^+$).

*1,3,5,7,9-Pentakis(4-N,N-dimethylanilinoethynyl)corannulene (**4**).* The mixture of 1,3,5,7,9-pentachlorocorannulene (550 mg, 1.3 mmol), $Pd(OAc)_2$ (147 mg, 0.65 mmol), IPr·HCl (556 mg, 1.3 mmol), and potassium *tert*-butoxide (146 mg, 1.3 mmol) in anhydrous dimethoxyethane

(50 mL) was stirred under N_2 at rt for 1 h. *N*,*N*-Dimethyl-4-[2-(trimethylstannyl)ethynyl]aniline (5 g, 15.71 mmol) was added to the solution and the mixture heated at reflux for 4 d. The solvent was evaporated and the residue purified by flash chromatography (FC) (SiO_2; CH_2Cl_2) to give compound **4** as an orange solid (380 mg, 30%). Mp: 310 °C dec. ^{1}H NMR (400 MHz, $CDCl_3$): δ = 3.03 (s, 30 H; N*Me*$_2$), 6.73 (d, *J* = 8.9 Hz, 10 H; *Ph*NMe$_2$), 7.61 (d, *J* = 8.9 Hz, 10 H; *Ph*NMe$_2$), 8.23 ppm (s, 5 H; corannulene). ^{13}C NMR (101 MHz, $CDCl_3$): δ = 40.4, 86.1, 95.8, 110.2, 112.1, 122.9, 129.7, 131.3, 133.3, 134.4, 150.5 ppm. IR (ATR): ν = 2887 (vw), 2855 (vw), 2799 (vw), 2176 (m), 1602 (s), 1519 (s), 1442 (m), 1352 (s), 1160 (s), 944 (m), 809 cm^{-1} (s). UV/vis (CH_2Cl_2): λ_{max} (ε) = 313 (114 100), 420 nm (86 300 M^{-1} cm^{-1}). HR-ESI-MS *m*/*z*: calcd for $C_{70}H_{56}N_5^+$ 966.45302, found 966.45278 ([M + H]$^+$); calcd for $C_{70}H_{57}N_5^{2+}$ 483.73015, found 483.72989 ([M + 2H]$^{2+}$).

*[3-[4-(Dimethylamino)phenyl]buta-1,3-diene-1,1,4,4-tetracarbonitrile-2-yl]corannulene (**5**).* Acetylene **1** (23 mg, 0.058 mmol) and TCNE (23 mg, 0.18 mmol) were dissolved in $(CHCl_2)_2$ (2 mL). The mixture was stirred at 25 °C for 1 h. The solvent was removed, and the residue was purified by FC (SiO_2; CH_2Cl_2) to give **5** as a red solid (29 mg, 96%). Mp: 190 °C dec. ^{1}H NMR (400 MHz, $CDCl_3$, 298 K): δ = 3.16 (s, 6 H; N*Me*$_2$), 6.75 (d, *J* = 9.3 Hz, 2 H; *Ph*NMe$_2$), 7.75 (d, *J* = 8.8 Hz, 1 H; corannulene), 7.79−7.94 (m, 8 H), 7.97 (d, *J* = 8.9 Hz, 1 H; corannulene), 8.06 ppm (d, *J* = 8.9 Hz, 1 H; corannulene). ^{13}C NMR (100 MHz, $CDCl_3$, 298 K): δ = 40.2, 74.9, 89.8, 111.7, 112.5, 112.8, 113.5, 114.5, 119.1, 125.8, 126.3, 127.1, 127.5, 128.3, 128.5, 129.1, 129.3, 131.5, 131.6, 131.8, 132.8, 133.7, 134.8, 135.7, 135.7, 137.1, 138.3, 154.5, 164.2, 167.3 ppm (30 out of 33 expected peaks). IR (ATR): ν = 3029 (vw), 2923 (vw), 2862 (vw), 2217 (m), 1604 (m), 1492 (m), 1385 (m), 1174 (m), 832 (m), 820 cm^{-1} (m). UV/vis (CH_2Cl_2): λ_{max} (ε) = 429 (26 100), 284 nm (28 100 M^{-1} cm^{-1}). HR-ESI-MS *m*/*z*: calcd for $C_{36}H_{19}N_5Na^+$ 544.15327, found 544.15359 ([M + Na]$^+$).

*2,5-Dimethyl-1,6-bis[3-[4-(dimethylamino)phenyl]buta-1,3-diene-1,1,4,4-tetracarbonitrile-2-yl]corannulene (**6**).* Diacetylene **2** (25 mg, 0.044 mmol) and TCNE (28 mg, 0.22 mmol) were dissolved in $(CHCl_2)_2$ (2.5 mL). The mixture was stirred at 25 °C for 2.5 h. The solvent was removed and the residue purified by FC (SiO_2; CH_2Cl_2/CH_3CN 1:0 → 40:1) to give **6** as a black solid with green luster (34 mg, 94%). Mp > 400 °C. ^{1}H NMR (500 MHz, CD_2Cl_2, 315 K): for isomer *a*, δ = 3.06 (s, 6 H; *Me*), 3.13 (s, 12 H; N*Me*$_2$), 6.77 (d, *J* = 8.5 Hz, 4 H; *Ph*NMe$_2$), 7.70 (d, *J* = 8.5 Hz, 4 H; *Ph*NMe$_2$), 7.75 (d, *J* = 4 Hz, 2 H; corannulene), 7.87 (d, *J* = 4 Hz, 2 H; corannulene), 8.09 ppm (s, 2 H; corannulene); for isomer *b*, δ = 3.06 (s, 6 H; *Me*), 3.12 (s, 12 H; N*Me*$_2$), 6.77 (d, *J* = 8.5 Hz, 4 H; *Ph*NMe$_2$), 7.70 (d, *J* = 8.5 Hz, 4 H; *Ph*NMe$_2$), 7.73 (d, *J* = 4 Hz, 2 H; corannulene), 7.89 (d, *J* = 4 Hz, 2 H; corannulene), 8.08 ppm (s, 2 H; corannulene); ^{13}C NMR (125 MHz, CD_2Cl_2, 300 K): for both isomers *a* and *b*, δ = 18.7, 40.59, 40.60, 80.2, 80.8, 97.2, 97.3, 111.6, 112.66, 112.71, 113.0, 113.2, 113.7, 113.9, 115.3, 115.4, 120.6, 120.8, 125.8, 125.9, 127.10, 127.13, 128.9, 129.0, 129.4, 129.5, 130.7, 130.9, 131.19, 131.22, 131.3, 133.7, 133.8, 135.1, 135.2, 135.7, 135.8, 135.99, 136.04, 142.3, 142.7, 155.0, 155.1, 165.1, 165.2, 167.7, 167.8 ppm (47 out of 50 expected peaks). IR (ATR): ν = 2919 (vw), 2859 (vw), 2809 (vw), 2211 (m), 1599 (m), 1481 (m), 1376 (m), 1169 (m), 817 cm^{-1} (m). UV/vis (CH_2Cl_2): λ_{max} (ε) = 600 (15600), 396 (30700), 301 nm (42200 M^{-1} cm^{-1}). HR-ESI-MS *m*/*z*: calcd for $C_{54}H_{32}N_{10}Na^+$ 843.27036, found 843.27025 ([M + Na]$^+$).

*1,3,5,7,9-Pentakis[3-[4-(dimethylamino)phenyl]buta-1,3-diene-1,1,4,4-tetracarbonitrile-2-yl]corannulene (**7**).* Pentaacetylene **4** (30 mg, 0.031 mmol) and TCNE (48 mg, 0.375 mmol) were dissolved in $(CHCl_2)_2$ (4 mL). The mixture was stirred at 25 °C for 16 h. The solvent was removed and the residue purified by FC (SiO_2; CH_2Cl_2/CH_3CN 40:1 → 15:1) to give **7** as a black solid with green luster (48 mg, 96%). Mp > 400 °C. ^{1}H NMR (500 MHz, $(CDCl_2)_2$, 410 K): δ = 3.22 (s, 30 H; N*Me*$_2$), 6.93 (d, *J* = 9.3 Hz, 10 H; *Ph*NMe$_2$), 7.83 (s, br, 5 H; corannulene), 8.07 ppm (d, br, 10 H; *Ph*NMe$_2$). ^{13}C NMR (125 MHz, $(CDCl_2)_2$, 410 K): δ = 39.6, 75.5, 91.5, 110.6, 112.5, 113.0, 113.7, 117.6, 126.6, 133.0, 133.1, 134.6, 136.5, 154.9, 160.1, 164.2 ppm (16 out of 17 expected peaks). IR (ATR): ν = 2920 (vw), 2864 (vw), 2807 (vw), 2214 (m), 1603 (m), 1492 (m), 1386 (m), 1173 (m), 820 cm^{-1} (m); UV/vis (CH_2Cl_2): λ_{max} (ε) = 600 (sh.), 468 (199 800), 363 nm (112 500 M^{-1} cm^{-1}). HR-ESI-MS *m*/*z*: calcd for $C_{100}H_{55}N_{25}Na^+$ 1628.49645, found 1628.49631 ([M + Na]$^+$). Anal. Calcd for $C_{100}H_{55}N_{25}$: C, 74.76; H, 3.45; N, 21.79. Found: C, 74.63; H, 3.75; N, 21.74.

*(E)-2-(2-(Corannulenyl)-1-(4-(dimethylamino)phenyl)-3-(4-(trifluoromethyl)phenyl)allylidene)malononitrile (**8**).* Acetylene **1** (23 mg, 0.058 mmol) and 2-[4-(trifluoromethyl)benzylidene]malononitrile (40 mg, 0.18 mmol) were dissolved in $(CHCl_2)_2$ (2 mL). The mixture was stirred at 120 °C for 2 d. The solvent was removed and the residue purified by FC (SiO_2; CH_2Cl_2) to give **8** as an orange solid (32 mg, 89%). Mp: 230−232 °C. ^{1}H NMR (500 MHz, CD_2Cl_2, 298 K): δ = 2.86 (s, 6 H; N*Me*$_2$), 6.50 (d, *J* = 9.3 Hz, 2 H; *Ph*NMe$_2$), 7.40 (d, *J* = 8.4 Hz, 2 H; *Ph*CF$_3$), 7.48 (d, *J* = 8.4 Hz, 2 H; *Ph*CF$_3$), 7.48 (s, 1 H, vinyl), 7.63 (d, *J* = 9.3 Hz, 2 H; *Ph*NMe$_2$), 7.65−7.71 (m, 4 H; corannulene), 7.74−7.84 ppm (m, 5 H; corannulene). ^{13}C NMR (125 MHz, CD_2Cl_2, 298 K): δ = 40.5, 78.2, 112.0, 115.7, 116.1, 121.1, 124.5 (q, *J* = 272.2 Hz, CF_3), 125.8 (q, *J* = 3.7 Hz, C_{ipso}-CF_3), 126.2, 127.3, 127.6, 127.8, 128.0, 128.1, 128.15, 128.21, 128.7, 129.8, 130.5, 130.7 (q, *J* = 32.5 Hz, C_{ortho}-CF_3), 131.2, 131.3, 131.7, 132.0, 132.8, 135.6, 135.7, 135.96, 136.03, 136.2, 136.7, 138.7, 139.1, 139.7, 153.4, 175.3 ppm. ^{19}F NMR (470 MHz, $CDCl_3$, 303 K): δ = −63.35 ppm (s, 3 F). IR (ATR): ν = 3029 (vw), 2918 (vw), 2857 (vw), 2216 (m), 1600 (m), 1497 (m), 1376 (m), 1320 (m), 1170 (m), 833 (m), 822 cm^{-1} (m). UV/vis (CH_2Cl_2): λ_{max} (ε) = 455 (21000), 297 nm (39500 M^{-1} cm^{-1}). HR-ESI-MS *m*/*z*: calcd for $C_{41}H_{25}F_3N_3^+$ 616.19951, found 616.19898 ([M + H]$^+$).

■ ASSOCIATED CONTENT

Ⓢ Supporting Information

Torsion angles of buta-1,3-dienes retrieved from Cambridge Structural Database (CSD), ^{1}H NMR of **8** at variable concentrations, ^{1}H VT-NMR of **5**, emission spectra of **1**−**4**, cyclic voltammetry of **7**, computational details, general and electrochemistry methods, and NMR spectra of new compounds. This material is available free of charge via the Internet at http://pubs.acs.org. The crystal structure data for **8** (CCDC 901534) is available from the Cambridge Crystallographic Data Centre via www.ccdc.cam.ac.uk/data_request/cif.

■ AUTHOR INFORMATION

Corresponding Author

*E-mail: (K.K.B.) kimb@oci.uzh.ch, (J.S.S.) jss@oci.uzh.ch, (F.D.) diederich@org.chem.ethz.ch.

Notes

The authors declare no competing financial interest.

■ ACKNOWLEDGMENTS

This work was supported by the ERC Advanced Grant No. 246637 (OPTELOMAC) and the Swiss National Science Foundation. We thank PD Dr. H. P. Lüthi (ETH) for valuable discussions about the properties of 2,3-diphenylbutadienes and Prof. B. Jaun (ETH) and Dr. B. Bernet (ETH) for valuable discussions about the conformations of compound **6**. Y.-L.W. is grateful for a fellowship from the Stipendienfonds der Schweizerischen Chemischen Industrie (SSCI). M.C.S. appreciates financial support from the Swiss National Science Foundation (Ambizione PZ00P2-126615).

■ REFERENCES

(1) (a) Coropceanu, V.; Cornil, J.; da Silva Filho, D. A.; Olivier, Y.; Silbey, R.; Brédas, J.-L. *Chem. Rev.* **2007**, *107*, 926−952. (b) Roncali, J.; Leriche, P.; Cravino, A. *Adv. Mater.* **2007**, *19*, 2045−2060. (c) Li, C.; Wonneberger, H. *Adv. Mater.* **2012**, *24*, 613−636.

(2) (a) Wu, Y.-T.; Siegel, J. S. *Chem. Rev.* **2006**, *106*, 4843−4867. (b) Tsefrikas, V. M.; Scott, L. T. *Chem. Rev.* **2006**, *106*, 4868−4884.

(3) (a) Seiders, T. J.; Baldridge, K. K.; Grube, G. H.; Siegel, J. S. *J. Am. Chem. Soc.* **2001**, *123*, 517−525. (b) Seiders, T. J.; Baldridge, K. K.; Siegel, J. S. *Tetrahedron* **2001**, *57*, 3737−3742. (c) Eisenberg, D.;

Filatov, A. S.; Jackson, E. A.; Rabinovitz, M.; Petrukhina, M. A.; Scott, L. T.; Shenhar, R. *J. Org. Chem.* **2008**, *73*, 6073−6078. (d) Bandera, D.; Baldridge, K. K.; Linden, A.; Dorta, R.; Siegel, J. S. *Angew. Chem., Int. Ed.* **2011**, *50*, 865−867.

(4) (a) Filatov, A. S.; Petrukhina, M. A. *Coord. Chem. Rev.* **2010**, *254*, 2234−2246. (b) Spisak, S. N.; Zabula, A. V.; Filatov, A. S.; Rogachev, A. Y.; Petrukhina, M. A. *Angew. Chem., Int. Ed.* **2011**, *50*, 8090−8094.

(5) (a) Gerald, R. E.; Klingler, R. J.; Sandi, G.; Johnson, C. S.; Scanlon, L. G.; Rathke, J. W. *J. Power Sources* **2000**, *89*, 237−243. (b) Kumar, T. P.; Kumari, T. S. D.; Stephan, A. M. *J. Indian Inst. Sci.* **2009**, *89*, 393−424. (c) Zabula, A. V.; Filatov, A. S.; Spisak, S. N.; Rogachev, A. Y.; Petrukhina, M. A. *Science* **2011**, *333*, 1008−1011.

(6) (a) Jones, C. S.; Elliott, E.; Siegel, J. S. *Synlett* **2004**, 187−191. (b) Mack, J.; Vogel, P.; Jones, D.; Kaval, N.; Sutton, A. *Org. Biomol. Chem.* **2007**, *5*, 2448−2452. (c) Wu, Y.-T.; Bandera, D.; Maag, R.; Linden, A.; Baldridge, K. K.; Siegel, J. S. *J. Am. Chem. Soc.* **2008**, *130*, 10729−10739. (d) Zoppi, L.; Martin-Samos, L.; Baldridge, K. K. *J. Am. Chem. Soc.* **2011**, *133*, 14002−14009.

(7) Valenti, G.; Bruno, C.; Rapino, S.; Fiorani, A.; Jackson, E. A.; Scott, L. T.; Paolucci, F.; Marcaccio, M. *J. Phys. Chem. C* **2010**, *114*, 19467−19472.

(8) (a) Michinobu, T.; Boudon, C.; Gisselbrecht, J.-P.; Seiler, P.; Frank, B.; Moonen, N. N. P.; Gross, M.; Diederich, F. *Chem.—Eur. J.* **2006**, *12*, 1889−1905. (b) Kivala, M.; Boudon, C.; Gisselbrecht, J. -P.; Seiler, P.; Gross, M.; Diederich, F. *Angew. Chem., Int. Ed.* **2007**, *46*, 6357−6360. (c) Kivala, M.; Diederich, F. *Acc. Chem. Res.* **2009**, *42*, 235−248. (d) Jarowski, P. D.; Wu, Y.-L.; Boudon, C.; Gisselbrecht, J.-P.; Gross, M.; Schweizer, W. B.; Diederich, F. *Org. Biomol. Chem.* **2009**, *7*, 1312−1322. (e) Wu, Y.-L.; Jarowski, P. D.; Schweizer, W. B.; Diederich, F. *Chem.—Eur. J.* **2010**, *16*, 202−211. (f) Kato, S.-i.; Diederich, F. *Chem. Commun.* **2010**, *46*, 1994−2006.

(9) (a) van Walree, C. A.; van der Wiel, B. C.; Jenneskens, L. W.; Lutz, M.; Spek, A. L.; Havenith, R. W. A.; van Lenthe, J. H. *Eur. J. Org. Chem.* **2007**, 4746−4751. (b) Limacher, P. A.; Luethi, H. P. *J. Phys. Chem. A* **2008**, *112*, 2913−2919.

(10) 2,3-Diarylated buta-1,3-dienes often adapt a synclinal conformation with torsion angle ∼65° in the crystal. See the Supporting Information for more details.

(11) Seiders, T. J.; Elliott, E. L.; Grube, G. H.; Siegel, J. S. *J. Am. Chem. Soc.* **1999**, *121*, 7804−7813.

(12) (a) Sygula, A.; Rabideau, P. W. *J. Am. Chem. Soc.* **2000**, *122*, 6323−6324. (b) Xu, G.; Sygula, A.; Marcinow, Z.; Rabideau, P. W. *Tetrahedron Lett.* **2000**, *41*, 9931−9934. (c) Sygula, A.; Xu, G. P.; Marcinow, Z.; Rabideau, P. W. *Tetrahedron* **2001**, *57*, 3637−3644.

(13) (a) Seiders, T. J.; Baldridge, K. K.; Elliott, E. L.; Grube, G. H.; Siegel, J. S. *J. Am. Chem. Soc.* **1999**, *121*, 7439−7440. (b) Grube, G. H.; Elliott, E. L.; Steffens, R. J.; Jones, C. S.; Baldridge, K. K.; Siegel, J. S. *Org. Lett.* **2003**, *5*, 713−716.

(14) Grasa, G. A.; Nolan, S. P. *Org. Lett.* **2001**, *3*, 119−122.

(15) (a) Chang, L. C. W.; von Frijtag Drabbe Künzel, J. K.; Mulder-Krieger, T.; Spanjersberg, R. F.; Roerink, S. F.; van den Hout, G.; Beukers, M. W.; Brussee, J.; Ijzerman, A. P. *J. Med. Chem.* **2005**, *48*, 2045−2053. (b) Silvestri, F.; Jordan, M.; Howes, K.; Kivala, M.; Rivera-Fuentes, P.; Boudon, C.; Gisselbrecht, J.-P.; Schweizer, W. B.; Seiler, P.; Chiu, M.; Diederich, F. *Chem.—Eur. J.* **2011**, *17*, 6088−6097.

(16) The molecule(s) isolated from column chromatography exhibit several Me and NMe_2 signals in the ^1H and ^{13}C NMR spectra ($(CDCl_2)_2$, 298−363 K), indicating more than one isomer. In the ^{13}C NMR spectrum ($CDCl_3$, 298 K), two peaks at 87.26 and 87.38 ppm were found, indicative of the presence of ethylene functionality. HR-ESI-MS *m*/*z* calcd for $C_{72}H_{49}N_{12}^{3+}$: 360.4729, found 360.4726 ([**3** + 2 TCNE + 3 H]$^{3+}$); calcd for $C_{72}H_{48}N_{12}^{2+}$: 540.2057, found 540.2051 ([**3** + 2 TCNE + 2 H]$^{2+}$); and calcd for $C_{72}H_{47}N_{12}^{+}$: 1079.4041, found 1079.4032 ([**3** + 2 TCNE + H]$^{+}$).

(17) Tahara, K.; Fujita, T.; Sonoda, M.; Shiro, M.; Tobe, Y. *J. Am. Chem. Soc.* **2008**, *130*, 14339−14345.

(18) Three examples showing similar arrangements of corannulenes, where an aliphatic group from one molecule located inside the concave face of corannulene from another molecule, were found by inspection in CSD: (a) Lee, H. B.; Sharp, P. R. *Organometallics* **2005**, *24*, 4875−4877. (b) Kobryn, L.; Henry, W. P.; Fronczek, F. R.; Sygula, R.; Sygula, A. *Tetrahedron Lett.* **2009**, *50*, 7124−7127. (c) Steinberg, B. D. Ph.D. Dissertation, Boston College, Chestnut Hill, MA, 2009.

(19) Schmidt, M. W.; Baldridge, K. K.; Boatz, J. A.; Elbert, S. T.; Gordon, M. S.; Jensen, J. H.; Koseki, S.; Matsunaga, N.; Nguyen, K. A.; Su, S. J.; Windus, T. L.; Dupuis, M.; Montgomery, J. A. *J. Comput. Chem.* **1993**, *14*, 1347−1363.

(20) (a) Weigend, F.; Ahlrichs, R. *Phys. Chem. Chem. Phys.* **2005**, *7*, 3297−3305. (b) Grimme, S. *J. Comput. Chem.* **2006**, *27*, 1787−1799. (c) Peverati, R.; Baldridge, K. K. *J. Chem. Theor. Comput.* **2008**, *4*, 2030−2048.

(21) (a) Gutowsky, H. S.; Holm, C. H. *J. Chem. Phys.* **1956**, *25*, 1228−1234. (b) Shanan-Atidi, H.; Bar-Eli, K. H. *J. Phys. Chem.* **1970**, *74*, 961−963. (c) Sandström, J. *Dynamic NMR Spectroscopy*; Academic Press: London; New York, 1982. (d) Ōki, M. *Applications of Dynamic NMR Spectroscopy to Organic Chemistry*; VCH Publishers: Deerfield Beach, FL, 1985.

(22) Yamada, M.; Rivera-Fuentes, P.; Schweizer, W. B.; Diederich, F. *Angew. Chem., Int. Ed.* **2010**, *49*, 3532−3535.

(23) Turro, N. J.; Ramamurthy, V.; Scaiano, J. C. *Modern Molecular Photochemistry of Organic Molecules*; University Science Books: Sausalito, CA, 2010.

(24) Frank, B. B.; Kivala, M.; Blanco, B. C.; Breiten, B.; Schweizer, W. B.; Laporta, P. R.; Biaggio, I.; Jahnke, E.; Tykwinski, R. R.; Boudon, C.; Gisselbrecht, J.-P.; Diederich, F. *Eur. J. Org. Chem.* **2010**, 2487−2503.

(25) Breiten, B.; Wu, Y.-L.; Jarowski, P. D.; Gisselbrecht, J.-P.; Boudon, C.; Griesser, M.; Onitsch, C.; Gescheidt, G.; Schweizer, W. B.; Langer, N.; Lennartz, C.; Diederich, F. *Chem. Sci.* **2011**, *2*, 88−93.

(26) (a) Folkers, E.; Runquist, O. *J. Org. Chem.* **1964**, *29*, 830−832. (b) Kurz, J. L.; Farrar, J. M. *J. Am. Chem. Soc.* **1969**, *91*, 6057−6062.

(27) (a) Seiders, T. J.; Baldridge, K. K.; Siegel, J. S.; Gleiter, R. *Tetrahedron Lett.* **2000**, *41*, 4519−4522. (b) Bruno, C.; Benassi, R.; Passalacqua, A.; Paolucci, F.; Fontanesi, C.; Marcaccio, M.; Jackson, E. A.; Scott, L. T. *J. Phys. Chem. B* **2009**, *113*, 1954−1962.

(28) $E_{1/2}$ = 0.40 V for Fc^+/Fc vs SCE (*n*-Bu_4NPF_6 in MeCN) was used to calibrate the reported potentials of corannulene. For other electrolyte/solvent systems, see: Connelly, N. G.; Geiger, W. E. *Chem. Rev.* **1996**, *96*, 877−910.

(29) (a) Keith, T. A.; Bader, R. F. W. *Chem. Phys. Lett.* **1993**, *210*, 223−231. (b) Cheeseman, J. R.; Trucks, G. W.; Keith, T. A.; Frisch, M. J. *J. Chem. Phys.* **1996**, *104*, 5497−5509.

(30) (a) Sheldrick, G. M. *Acta Cryst. A* **2008**, *64*, 112−122. (b) Dolomanov, O. V.; Bourhis, L. J.; Gildea, R. J.; Howard, J. A. K.; Puschmann, H. *J. Appl. Crystallogr.* **2009**, *42*, 339−341.